Novel superhydrophobic microporous layers for enhanced performance and efficient water management in PEM fuel cells

Saverio Latorrata[*], *Paola Gallo Stampino*, *Cinzia Cristiani*, *Giovanni Dotelli*

Department of Chemistry, Materials and Chemical Engineering "Giulio Natta", Politecnico di Milano, Piazza Leonardo da Vinci 32, 20133 Milan, Italy

Received 30 September 2013
Received in revised form
20 December 2013
Accepted 28 December 2013
Available online 20 January 2014

1. Introduction

Proton exchange membrane fuel cells (PEMFCs) are attractive as an alternative power source for both automotive and stationary applications, because of their capability of producing high power densities and to undergo rapid changes in load [1–5]. An efficient water management [6] is fundamental to obtain enough power, to prevent degradation of materials and to avoid flooding of the electrodes. In fact, a deficiency in water amount inside the cell would result in reduction of ionic conductivity of the membrane as well as it would drive to severe contact resistances between the membrane and the catalyst layer. On the other hand, excess water would cause diffusive limitations thus reducing catalytic sites for electrochemical reactions and hindering reactants transport to the electrodes [7–11]. Gas Diffusion Medium (GDM), which consists of a microporous layer (MPL) coated onto a carbon fibre-based macroporous substrate (Gas Diffusion Layer, GDL), is able to manage water. GDM is electrically conductive and guarantees an efficient contact between catalyst layer and bipolar plate. An optimal GDM allows to reduce flooding under high relative humidity (RH) conditions and to prevent membrane dehydration under low RH conditions [11–14]. Gas Diffusion Layer (GDL) can be a carbon-based cloth placed between the gas flow channels and the catalyst layer. Its characteristics such as thickness, porosity, hydrophobicity and permeability play a crucial role in determining the water

* *Corresponding author*. Tel.: +39 02 23993233; fax: +39 02 70638173.
E-mail address: saverio.latorrata@polimi.it (S. Latorrata).

management efficiency during PEMFC operations [10,15–18]. MPL is composed of carbon particles and of a hydrophobic polymeric binder: due to its microporosity, it improves water removal capability. Many studies have demonstrated that a microporous layer coated onto the GDL is effective in improving water management, thereby getting better electrical performances [8,10–12,14,16,19,20]. Indeed, MPL acts as a valve that pushes water away from the catalyst layer to the flow field to lower water saturation level [20–22]. A more hydrophobic MPL would allow faster water removal from the cathode side [23]. A classical MPL formulation mainly contains carbon black (CB), polytetrafluoroethylene (PTFE) as both binder and hydrophobic agent. CB is dispersed using proper solvents and dispersants; a PTFE suspension is then added. This resulting ink is deposited onto one side of the GDL substrate pretreated with PTFE and the so formed GDM is then heat treated to evaporate solvents and surfactants and to sinter the hydrophobic polymer [10].

The effect on water management of the different MPL components has been extensively investigated during the last decade [10] and carbon powder quality, wettability, carbon loading, thickness and porosity were suggested to be responsible for the final MPL properties. Much less attention has been paid on the nature of the hydrophobic agent, keeping PTFE as the best choice for that purpose for many years. Some works have dealt with the employment of different polymers such as fluorinated ethylene propylene (FEP) [24,25] and polyvinylidene fluoride (PVDF) [26]. However, they were proposed only to treat GDLs to make them more hydrophobic than PTFE-based substrates and also some of us have recently reported the beneficial effects of the use of perfluoropolyether (PFPE) derivatives for hydrophobic surface treatments of GDLs [27]. However, only few works report the use of polymers other than PTFE in inks formulation for MPLs hydrophobization [28–30].

In the present study, three different polymers were used in order to replace PTFE, namely perfluoroalcoxy (PFA), fluorinated ethylene propylene (FEP) and a fluorinated polyurethane (Fluorolink® P56, Solvay) based on perfluoropolyether (PFPE) blocks [31–35]. Proper formulations were prepared and the effect of the polymers nature on the rheological behaviour of the ink was studied. The final MPL properties, in terms of static contact angle values and morphology, were investigated. The electrical behaviour of a cell containing such innovative MPLs was assessed by polarization curves, power density curves and impedance spectroscopy at 60 °C and two different cathodic RHs (100 and 60%).

2. Experimental

2.1. *Preparation*

Commercial carbon cloths (S5, from SAATI, Italy) were used as GDLs [36,37]. Three commercial aqueous dispersions of polymers as hydrophobic agents were used: a high molecular perfluoropolyether (PFPE) Fluorolink® P56 from Solvay Solexis, fluorinated ethylene propylene (FEP) and perfluoroalcoxy (PFA) both from DuPont. Before coating deposition, GDLs were hydrophobized by dipping in a solution containing 1% wt of the selected fluorinated polymer for 20 min. Subsequently, they were treated in air for 30 min up to 150, 260 and 305 °C to sinter PFPE, FEP and PFA, respectively. The temperatures chosen for FEP and PFA are those recommended by the manufacturing company (DuPont) of polymers, in order to reach a temperature close to their melting points. Whereas, unlike FEP and PFA, which are semi-crystalline, PFPE is amorphous and it has not any melting point. Thus, the selected temperature for treating it (150 °C) is to be intended just to eliminate solvents and surfactants after preparation of the MPL.

Highly conductive graphitic carbon black (CB, Cabot Vulcan XC72R) with high surface area was used for MPL preparation. Isopropyl alcohol (IPA), supplied by Sigma–Aldrich, was used as solvent and dispersant. Slurry composition and experimental procedures were selected according to Refs. [10,13].

In a typical experiment, a solution of polymer dispersion and IPA in deionized water was prepared and CB was slowly added. The mixture was vigorously stirred and homogenized by a high shear mixer (UltraTurrax T25) at 8000 rpm for 10 min. The following inks compositions were selected: CB/$H_2O = 0.13$ [w/w], Fluorinated Polymer/CB = 0.12 [w/w] and CB/IPA = 5.6 [w/w].

This formulation would guarantee a proper rheological behaviour of the ink when used in blade coating procedure. Indeed, the inks obtained were deposited onto the hydrophobized GDL substrates via the blade coating technique, using a lab-scale commercial equipment K-101 Control Coater. A linear velocity of 0.0154 m/s and a 40 μm gap, corresponding to a shear rate of about 350 s^{-1}, were adopted.

Finally, to remove water, IPA and to sinter the fluorinated polymer used in the formulation, the coated samples were calcined up to 150, 260 and 305 °C for PFPE, FEP and PFA, respectively.

2.2. *Characterization*

The rheological behaviour of the obtained inks was tested at 20 °C by means of a rotational rheometer (Rheometrics DFR 200) equipped with a 40 mm parallel-plates geometry, with a gap between the stationary plate and the movable one of 1 mm. Dynamic viscosities were investigated in the shear rates range $10^{-3} \div 10^{3}$ s^{-1}.

Static contact angles of the GDMs were measured according to the sessile drop technique, using an OCA 20 Dataphysics Instrument. Values reported in this paper are the result of the average of ten measurements.

A Cambridge Stereoscan 360 scanning electron microscope (SEM) was used for the morphological analyses of GDMs. SEM analyses were carried out both onto the surfaces and the cross-sections of the samples, which were gold coated to prevent charging effects.

The electrochemical performances of the four GDMs were tested in a single lab-scale cell in terms of polarization, power density curves and electrochemical impedance spectroscopy (EIS).

GDLs coated by MPLs were added both to the anodic side and to the cathodic one. Graphitic bipolar plates, with a single serpentine at the anode and a triple one at the cathode, were used. A commercial Catalyst Coated Membrane (CCM, supplied by Baltic Fuel Cells), which consists of catalyst layers (active

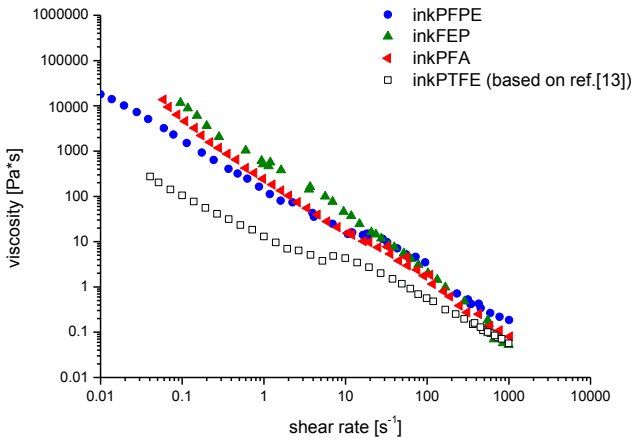

Fig. 1 – Flow curves of the inks containing the different polymers. PTFE-based ink (white squares) refers to preparation and measurements performed in Ref. [13].

area of 23 cm^2) directly coated onto a 50 μm thick Nafion membrane, was employed as MEA. The platinum loading was 0.3 mg cm^{-2} at the anode and 0.6 mg cm^{-2} at the cathode.

Calibrated flows of hydrogen and air were fed to the anode and the cathode, respectively. Stoichiometric ratio λ (calculated at 25 A) was 1.2 for hydrogen and 2.4 for air. Inlet gas humidity and temperature were controlled by external humidifiers and temperature controllers.

Experiments were carried out at 60 °C under two different relative humidity (RH) conditions of air feeding, namely 60 and 100%, whereas the hydrogen RH was fixed at 80%. Voltage, current and generated power were measured with an electronic load (RBL488-50-150-800) connected to the cell.

Polarization curves were recorded under galvanostatic conditions in the current density range from OCV to 1.13 A/cm^2, with steps of 0.09 A/cm^2. In the same range, EIS was carried out using a Frequency Response Analyzer (FRA, Solartron 1260). All spectra were obtained over a frequency range of 0.5 Hz–1 kHz (10 points per decade). At each current density, five experimental spectra were acquired and averaged to obtain the spectrum reported in the Nyquist diagram. All the experimental data were fitted using the Zview® software (Scribner Associates) by using equivalent circuits made of a resistance (Rs) in series with two parallel capacitance/resistance circuits, (Rp/Cdl) and (Rd/Cd). Rs represents the ohmic losses, while the first circuit (Rp/Cdl) models the activation polarization (i.e. charge transfer resistance) and the second one (Rd/Cd) models the losses related to the concentration polarization and flooding phenomena (i.e. mass transfer resistance) [36–39]. Actually, constant phase elements (CPE) were used instead of pure capacitances to account for the capacitive losses that generally occur in porous electrodes [40,41].

3. Results and discussion

3.1. *Inks rheological behaviour*

Pseudo-plastic shear thinning fluids are desirable for blade coating processes [42,43]. Fig. 1 shows the flow curves of the three different inks and that of the PTFE-based ink composition. Independently on the nature of the polymer, all the samples are pseudo-plastic, showing a viscosity which decreases on increasing the shear rate.

The three curves related to innovative inks become very similar at shear rates higher than 100 s^{-1}, typical shear rate values employed for blade coating technique.

The rheological behaviour of similar ink compositions, but based on PTFE, has been already reported [13,43]. In that case, a final coating layer about 65 μm thick was obtained when deposition was performed at a shear rate of about 100 s^{-1}. In the case of the fluorinated polymers here studied, viscosity values somewhat higher than those reported for PTFE are found. Thus, considering that the layer thickness is a combination of viscosity and shear rate, to obtain a comparable thickness among PFPE, PFA, FEP and PTFE, the deposition procedure was operated fixing the shear rate at about 350 s^{-1}.

3.2. *Surface characterization*

SEM images of hydrophobized GDLs and GDMs surface and their cross-section are reported in Fig. 2((a,b,c) FEP, (d, e, f) PFA, (g, h, i) PFPE and (l, m, n) PTFE). The GDLs surfaces (a, d, g, l), upon hydrophobization and thermal treatment, showed the presence of a homogeneous distribution of the polymeric matter around the GDLs fibres, suggesting that the hydrophobization procedure was successful.

The images of the final MPL coatings, reported in Fig. 2 (b, e, h, m), highlight smooth and quite homogeneous surfaces for all the samples, even though traces of the fibres of the bare GDL are still evident, mainly in the PFPE-containing MPL. Furthermore, also identifiable cracks, of variable dimensions, are found at the surface of all the samples. The presence of cracks is always reported in the literature to form upon thermal treatment due to typical shrinkage phenomena during solvent elimination. In principle, cracks formation has to be hampered because it could result in coating shedding during the cell operation. However, if the phenomenon of cracks formation is limited to the layer surface, e.g. less deep cracks are formed, the coating detachment is negligible.

3.3. *Contact angle*

Contact angle measurements give an indication of the hydrophobicity of the GDMs (Fig. 3). All the prepared GDMs are more hydrophobic than PTFE-containing samples [13]. A superhydrophobic surface, namely an average contact angle higher than 150°, was obtained for FEP-containing MPL. These values could indicate a different behaviour of the surfaces in terms of water management: the higher is the contact angle the faster the water removal should be.

3.4. *Electrochemical performances*

The steady-state current density–potential curves of the PEMFC assembled with the three different types of GDM are reported in Fig. 4. For the sake of comparison, polarization curves obtained with traditional PTFE-based GDMs are also reported. The results hereafter presented correspond to the

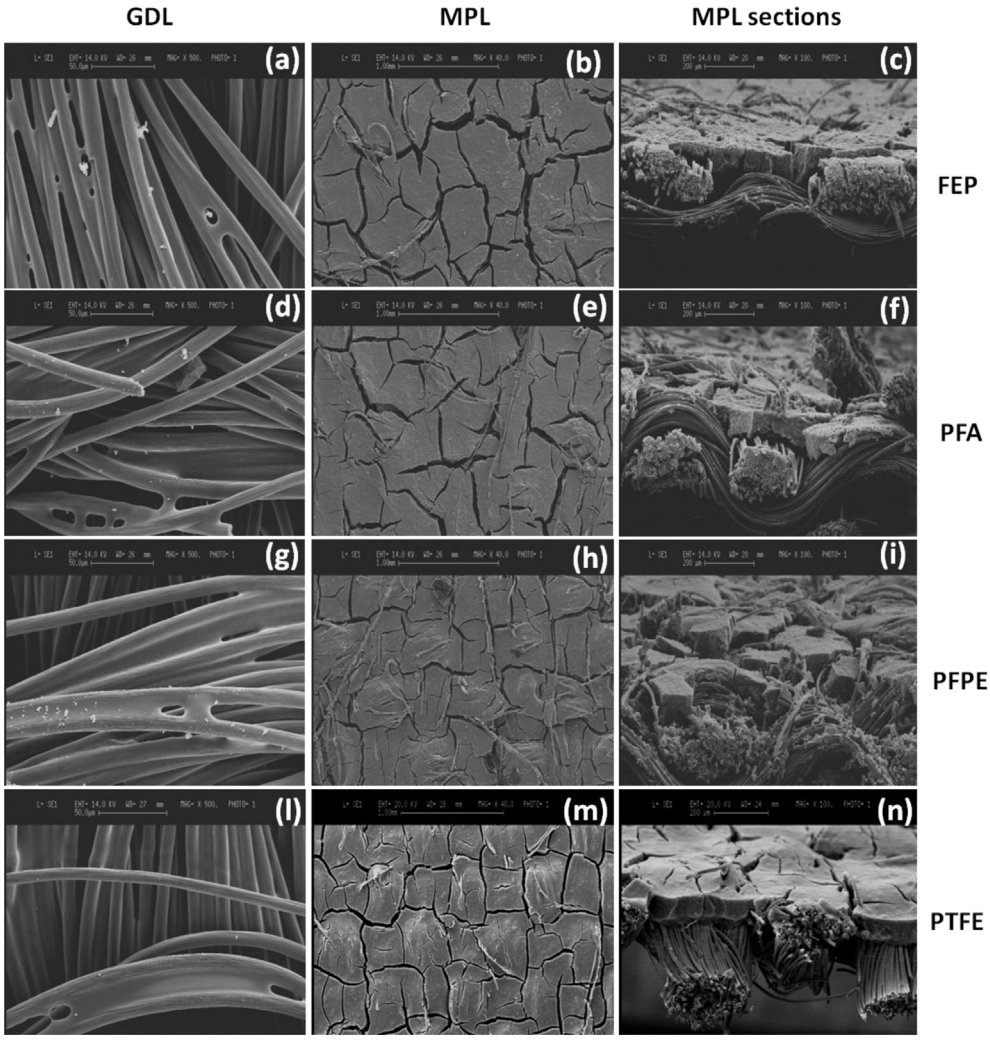

Fig. 2 – SEM images of GDL fibres (a, d, g, l, 500×), MPL surfaces (b, e, h, m, 40×) and MPL sections (c, f, i, n, 100×) of samples containing FEP (a, b, c), PFA (d, e, f), PFPE (g, h, i) and PTFE (l, m, n).

early experiments on these innovative materials, but first replies (on FEP-based GDMs) have already confirmed such tests.

All the new samples were able to improve the electrical performance with respect to that showed by the cell assembled with classical GDMs based on PTFE. In particular, the presence of FEP drives to a significant improvement, above all at high cathodic RH (Fig. 4(a)), while at low cathodic RH (Fig. 4(b)) PFPE-containing GDMs compare well with those based on FEP, at least both reach more or less the same value of the maximum power density. However, when cathodic RH is reduced to 60% (Fig. 4(b)), only the PFPE-containing MPLs showed an increase of the maximum power density reached.

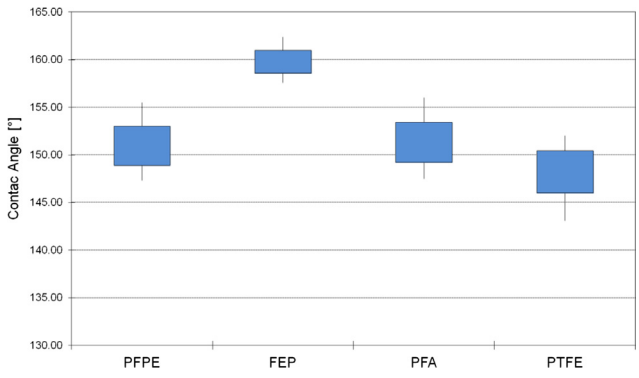

Fig. 3 – Results of the contact angle analysis on the four surfaces investigated.

The typical impedance spectra of a running fuel cell under low current density (0.19 A/cm^2), medium current density (0.47 A/cm^2) and high current density (0.86 A/cm^2) are shown in Fig. 5 for both RHs employed and for all the samples prepared.

It can be noticed that, at low current density, for all samples and both operating conditions, the impedance spectrum shows just one arc, arising from the activation polarization process, while at medium and at high current density, even more clearly pronounced, two arcs are observed: the higher frequency arc (left) corresponds to the polarization process due to charge transfer limitations and the lower frequency

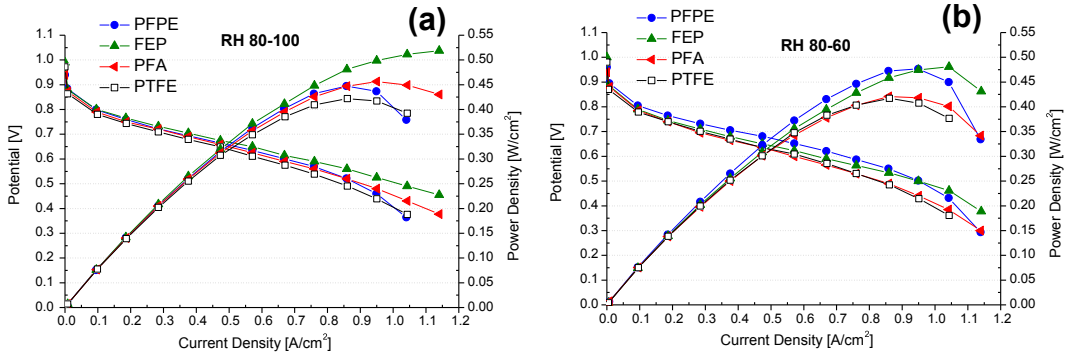

Fig. 4 – Polarization and power density curves of the running fuel cells assembled with the four GDMs at 60 °C and RH 80–100 (a) and RH 80–60 (b).

one (right) deals with the diffusion issues caused by mass transfer limitations [38].

The trends of Rs and Rd parameters obtained by fitting, using the equivalent circuits discussed in the experimental section, are reported in Fig. 6 as a function of current density for both RH conditions. Features and efficiency of the GDMs influenced mostly Rs and Rd, while Rp parameter is generally more related to catalytic activity and keeps almost constant when current density is increasing. For this reason we reported only data about Rs and Rd parameters.

It is evident that when RH is high (Fig. 6(a)) Rs keeps quasi-constant with increasing current density, while at 60% of cathodic RH (Fig. 6(b)) it is higher at low current density values because of the weak membrane hydration when system is near OCV (i.e. very low current density) and so no water is generated. PFPE-based samples show the lower ohmic resistance in the whole current densities range and at both RH conditions. Rd is strictly related to mass transfer limitations and depends on the water amount between the catalyst layer and MPL, so GDM water management ability is best revealed in Fig. 6(c) and (d) showing Rd vs current density. As expected, Rd increases dramatically with current density, especially at high RH (Fig. 6(c)), but FEP- and PFA- based MPLs can manage quite well the increasing amount of water if compared with PTFE-MPLs; on the contrary, this is not the case for PFPE-containing MPLs.

Table 1 may help to summarize the main results, in terms of electrochemical parameters and contact angles, and to discuss them in this section.

The results of the electrochemical tests can be related to wettability and hydrophobicity of the prepared MPLs. Indeed, FEP-based samples have a strong superhydrophobic behaviour, i.e. a contact angle higher than 160°, and clearly superior to that of all other samples whose contact angles are, instead, all around 150°. This feature is probably the main reason behind the very good electrochemical performance, especially

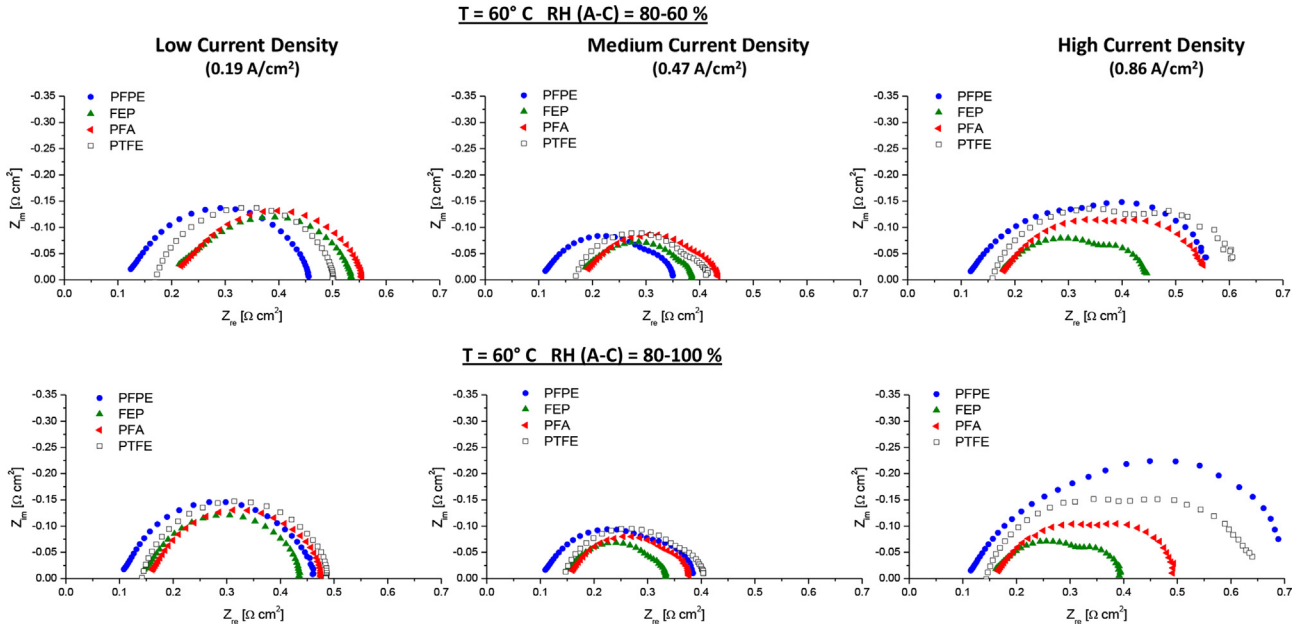

Fig. 5 – Examples of impedance spectra obtained at low, medium and high current density for fuel cells assembled with the four GDMs, running at 60 °C and RH 80–60 and RH 80–100.

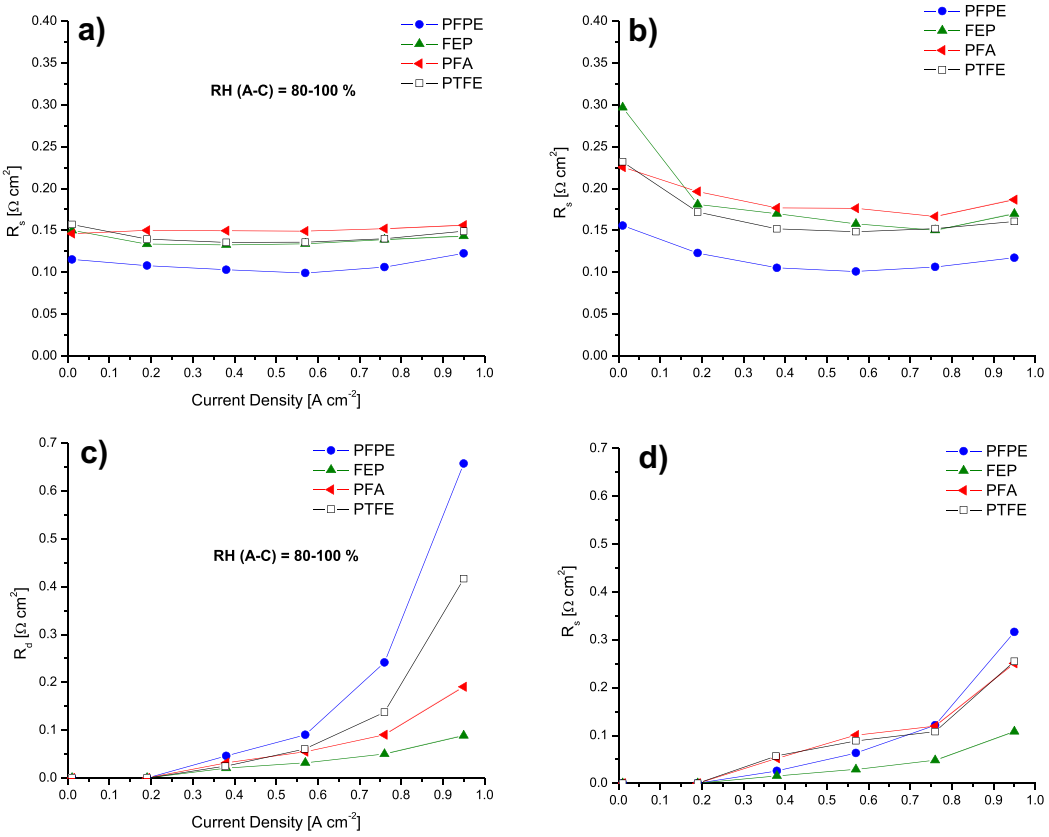

Fig. 6 – Trends of R_s and R_d parameters as a function of current density at high (a, c) and low (b, d) relative humidity.

at high current densities; indeed, FEP-containing MPLs show the maximum power density and the minimum mass transfer resistance Rd (Table 1). Considering that the performances are even better at high RH, it is clear that the presence of FEP leads to a better management of water, even in conditions of high cathodic RH, i.e. saturation of inlet feeding air. PFA-based MPLs have the same positive trend as GDM-FEP (increase of P_{max} and decrease of Rd when air is saturated), but less pronounced. GDM-PTFE have also this behaviour, but less performing.

On the contrary, PFPE-based GDMs showed a better performance when cathodic RH is low (Fig. 4(b)), clearly in contrast with the behaviour of the other polymer-based cells and conflicting with expectations. The water management ability of these GDMs is doubtful, at least based on the outcomes of electrochemical performances: the ohmic resistance Rs is very low (about 100 mΩ cm^2 vs 150 for all other samples) and insensitive of the air RH (Table 1); the mass transfer resistance Rd is very large and it almost doubles upon increasing RH; the maximum power density is better at low RH. The comprehension of this behaviour is not straightforward, especially considering that the contact angle is of the same order of magnitude as PFA and PTFE-MPLs; however, a possible explanation could be related to the imperfect adhesion of the MPL to the GDL substrate, an occurrence which would cause detachment of MPL portions when more water is fed (i.e. high cathodic RH). Indeed, PFPE is an amorphous polymer, so it has not a melting point and a proper sintering temperature. This feature could explain the faulty adhesion of the whole MPL surface to the substrate. However, the very good performance at low RH in terms of polarization curve and maximum power density makes PFPE a good candidate for cell operating in low-humidity conditions, even if much work must be done to improve the lifetime of the MPL.

All in all, GDM-FEP represents a clear improvement with respect to state-of-the-art PTFE-GDM; GDM-PFA too performs

Table 1 – Main results of the tests: contact angle, maximum power density reached, minimum ohmic resistance and maximum diffusion resistance measured for all the samples both at cathodic RH 100% and 60%.

Sample	Contact angle [°]	P_{max} (RH100) [mW/cm^2]	P_{max} (RH60) [mW/cm^2]	$R_{s,min}$ (RH100) [mΩ cm^2]	$R_{s,min}$ (RH60) [mΩ cm^2]	$R_{d,max}$ (RH100) [mΩ cm^2]	$R_{d,max}$ (RH60) [mΩ cm^2]
GDM-PFPE	150 ± 3	449	475	99	101	657	316
GDM-FEP	160 ± 2	517	481	133	150	89	108
GDM-PFA	154 ± 3	456	422	146	167	191	251
GDM-PTFE	149 ± 3	421	416	136	149	416	255

well, especially at high RH. Moreover, both polymers enhance the cell behaviour upon increasing RH, an occurrence which reveals a good water management ability, certainly superior to that of PTFE-based MPLs. On the contrary, PFPE is not very effective in water removal, even though its performances are absolutely comparable with those of GDM-PTFE at high RH, and much better at low RH.

4. Conclusions

Gas Diffusion Media should improve the contact between catalyst layer and bipolar plate leading to an increase of fuel cell efficiency. Moreover it has to be hydrophobic in order to guarantee the fast removal of water produced by cathodic reduction reaction.

Three different kinds of MPL were manufactured using PFPE, FEP and PFA in order to replace traditional PTFE-based gas diffusion media, aiming to enhance hydrophobicity and electrochemical performances of the whole fuel cell system. Moreover, such polymers have a lower sintering temperature with respect to PTFE.

The addition of these polymers did not change significantly rheological properties (with respect to inks containing PTFE) of the slurries used to prepare MPLs, allowing to obtain pseudo-plastic fluids, suitable for blade coating technique.

FEP-based MPLs showed a superhydrophobic surface that led to reduce significantly mass transfer limitations, both at low and high RH. As a consequence, cell performances are enhanced: the fuel cell assembled with GDMs containing FEP reached the highest power density. Thus, FEP could already be considered as a reasonable alternative to PTFE in GDMs fabrication. However, investigations on the durability of such innovative promising materials are necessary as well as studies which would help to understand the eventual mechanisms of degradation with the aim of reducing and/or eliminating it. Moreover, different amounts of polymer, in particular FEP which showed the best findings, could be assessed, aiming to reach the best compromise between polymer amount and global resistance of the whole system.

REFERENCES

[1] Stone C. From curiosity “to power to change the world”. Solid State Ion 2002;152:1–13.
[2] Perry ML, Fuller TF. A historical perspective of fuel cell technology in the 20th century. J Electrochem Soc 2002;149:S59–67.
[3] Wee J. Applications of proton exchange membrane fuel cell systems. Renew Sustain Energy Rev 2007;11:1720–38.
[4] Venturelli L, Santangelo PE, Tartarini P. Fuel cell systems and traditional technologies. Part II: experimental study on dynamic behavior of PEMFC in stationary power generation. Appl Therm Eng 2009;29:3469–75.
[5] Barbir F. PEM fuel cells: theory and practice. Amsterdam: Elsevier Academic Press; 2005.
[6] Dai W, Wang H, Yuan X-Z, Martin JJ, Yang D, Qiao J, et al. A review on water balance in the membrane electrode assembly of proton exchange membrane fuel cells. Int J Hydrogen Energy 2009;34:9461–78.
[7] Jung UH, Jeong SU, Park KT, Lee HM, Chun K, Choi DW, et al. Improvement of water management in air-breathing and air-blowing PEMFC at low temperature using hydrophilic silica nano-particles. Int J Hydrogen Energy 2007;32:4459–65.
[8] Chen J, Matsuura T, Hori M. Novel gas diffusion layer with water management function for PEMFC. J Power Sources 2004;131:155–61.
[9] Park GG, Sohn YJ, Yang TH, Yoon YG, Lee WY, Kim CS. Effect of PTFE contents in the gas diffusion media on the performance of PEMFC. J Power Sources 2004;131:182–7.
[10] Park S, Lee JW, Popov BN. A review of gas diffusion layer in PEM fuel cells: materials and designs. Int J Hydrogen Energy 2012;37:5850–65.
[11] Kim T, Lee S, Park H. A study of water transport as a function of the micro-porous layer arrangement in PEMFCs. Int J Hydrogen Energy 2010;35:8631–43.
[12] Kitahara T, Konomi T, Nakajima H. Microporous layer coated gas diffusion layers for enhanced performance of polymer electrolyte fuel cells. J Power Sources 2010;195:2202–11.
[13] Latorrata S, Stampino PG, Amici E, Pelosato R, Cristiani C, Dotelli G. Effect of rheology controller agent addition to micro-porous layers on PEMFC performances. Solid State Ionics 2012;216:73–7.
[14] Kitahara T, Nakajima H, Mori K. Hydrophilic and hydrophobic double microporous layer coated gas diffusion layer for enhancing performance of polymer electrolyte fuel cells under no-humidification at the cathode. J Power Sources 2012;199:29–36.
[15] Kandlikar SG, Garofalo ML, Lu Z. Water Management in A PEMFC: water transport mechanism and material degradation in gas diffusion layers. Fuel Cells 2011;11:814–23.
[16] Williams MV, Begg E, Bonville L, Kunz HR, Fenton JM. Characterization of gas diffusion layers for PEMFC. J Electrochem Soc 2004;151:A1173–80.
[17] Zheng WY, Zhu DS, Zhou GY, Wu JF, Shi YY. Thermal performance analysis of closed wet cooling towers under both unsaturated and supersaturated conditions. Int J Heat Mass Transf 2012;55:7803–11.
[18] Zhou ZF, Wu WT, Chen B, Wang GX, Guo LJ. An experimental study on the spray and thermal characteristics of R134a two-phase flashing spray. Int J Heat Mass Transf 2012;55:4460–8.
[19] Pasaogullari U, Wang CY. Liquid water transport in gas diffusion layer of polymer electrolyte fuel cells. J Electrochem Soc 2004;151:A399–406.
[20] Weber AZ, Newman J. Effects of microporous layers in polymer electrolyte fuel cells. J Electrochem Soc 2005;152:A677–88.
[21] Wu R, Liao Q, Zhu X, Wang H. Liquid and oxygen transport through bilayer gas diffusion materials of proton exchange membrane fuel cells. Int J Heat Mass Transf 2012;55:6363–73.
[22] Chun JH, Jo DH, Kim SG, Park SH, Lee CH, Kim SH. Improvement of the mechanical durability of micro porous layer in a proton exchange membrane fuel cell by elimination of surface cracks. Renew Energy 2012;48:35–41.
[23] Park S, Popov BN. Effect of hydrophobicity and pore geometry in cathode GDL on PEM fuel cell performance. Electrochim Acta 2009;54:3473–9.
[24] Lim C, Wang CY. Effects of hydrophobic polymer content in GDL on power performance of a PEM fuel cell. Electrochim Acta 2004;49:4149–56.
[25] Borup RL, Davey JR, Garzon FH, Wood DL, Inbody MA. PEM fuel cell electrocatalyst durability measurements. J Power Sources 2006;163:76–81.
[26] Cabasso I, Yuan Y, Xu X. Gas diffusion electrodes based on poly(vinylidene fluoride) carbon blends US Patent No. 5783325. 1998.
[27] Stampino PG, Latorrata S, Molina D, Turri S, Levi M, Dotelli G. Investigation of hydrophobic treatments with

perfluoropolyether derivatives of gas diffusion layers by electrochemical impedance spectroscopy in PEM-FC. Solid State Ionics 2012;216:100–4.
[28] Yan WM, Wu DK, Wang XD, Ong AL, Lee DJ, Su A. Optimal microporous layer for proton exchange membrane fuel cell. J Power Sources 2010;195:5731–4.
[29] Park SB, Park YI. Fabrication of gas diffusion layer (GDL) containing microporous layer using flourinated ethylene prophylene (FEP) for proton exchange membrane fuel cell (PEMFC). Int J Precis Eng Man 2012;13:1145–51.
[30] Purwanto WW, Slamet, Wargadalam VJ, Pranoto B. Effects of the addition of flourinated polymers and carbon nanotubes in microporous layer on the improvement of performance of a proton exchange membrane fuel cell. Int J Electrochem Sci 2012;7:525–33.
[31] Licchelli M, Marzolla SJ, Poggi A, Zanchi C. Crosslinked fluorinated polyurethanes for the protection of stone surfaces from graffiti. J Cult Herit 2011;12:34–43.
[32] Jiang M, Zhao XL, Ding XB, Zheng ZH, Peng YX. A novel approach to fluorinated polyurethane by macromonomer copolymerization. Eur Polym J 2005;41:1798–803.
[33] Stobie N, Duffy B, Hinder SJ, McHale P, McCormack DE. Silver doped perfluoropolyether-urethane coatings: antibacterial activity and surface analysis. Colloid Surf B 2009;72:62–7.
[34] Trombetta T, Iengo P, Turri S. Fluorinated segmented polyurethane anionomers for water-oil repellent surface treatments of cellulosic substrates. J Appl Polym Sci 2005;98:1364–72.
[35] Jones B. Fluoropolymers for coating applications. Jct Coatingstech 2008;5:44–8.
[36] Omati L, Stampino PG, Dotelli G, Brivio D, Grassini P. Operative conditions effect on PEM-FC performance by in-situ and ex-situ analysis of gas diffusion media with different bulk textile structure. Int J Hydrogen Energy 2011;36:8053–62.
[37] Dotelli G, Omati L, Stampino PG, Grassini P, Brivio D. Investigation of gas diffusion layer compression by electrochemical impedance spectroscopy on running polymer electrolyte membrane fuel cells. J Power Sources 2011;196:8955–66.
[38] Asghari S, Mokmeli A, Samavati M. Study of PEM fuel cell performance by electrochemical impedance spectroscopy. Int J Hydrogen Energy 2010;35:9283–90.
[39] Wagner N. Characterization of membrane electrode assemblies in polymer electrolyte fuel cells using a.c. impedance spectroscopy. J Appl Electrochem 2002;32:859–63.
[40] Ramasamy RP, Kumbur EC, Mench MM, Liu W, Moore D, Murthy M. Investigation of macro- and micro-porous layer interaction in polymer electrolyte fuel cells. Int J Hydrogen Energy 2008;33:3351–67.
[41] Dhirde AM, Dale NV, Salehfar H, Mann MD, Han TH. Equivalent electric circuit modeling and performance analysis of a PEM fuel cell stack using impedance spectroscopy. Ieee T Energy Conver 2010;25:778–86.
[42] Tracton AA. Coatings materials and surface coatings. Boca Raton, FL: CRC Press; 2007.
[43] Stampino PG, Cristiani C, Dotelli G, Omati L, Zampori L, Pelosato R, et al. Effect of different substrates, inks composition and rheology on coating deposition of microporous layer (MPL) for PEM-FCs. Catal Today 2009;147:S30–5.